FULL PAPER

Solvent Effect on the NMR Chemical Shieldings in Water Calculated by a Combination of Molecular Dynamics and Density Functional Theory

Vladimir G. Malkin,* Olga L. Malkina, Gerold Steinebrunner, and Hanspeter Huber*

Abstract: The solvent effect on the NMR chemical shielding in liquid water is calculated from a combination of molecular dynamics simulations and quantum chemical calculations for protons and ^{17}O. The simulations are performed with three different potentials, ab initio as well as empirical ones, to study the influence of the force field. From the liquid configurations obtained in these simulations, molecules are randomly chosen together with neighbouring molecules to give clusters of water typical for the liquid at the selected temperature and density. Different cluster sizes are studied. The clusters are treated as supermolecules in quantum chemical calculations of chemical shifts by sum-over-states density functional perturbation theory with individual gauge for localised orbitals. The influence of the quantum chemical method is studied with

Keywords

density-functional theory · liquid water · molecular dynamics simulations · NMR chemical shifts · solvent effects

an ab initio coupled Hartree–Fock gauge including atomic orbitals calculations with different basis sets for a selected cluster. An average over clusters yields the chemical shielding in the liquid at the selected temperature and density. The calculated values for the gas–liquid shift, which are in best agreement with experiment, are −3.2 ppm (exp. −4.26 ppm) for the proton and −37.6 ppm (exp. −36.1 ppm) for ^{17}O, but the results depend strongly on the chosen interatomic potential.

Introduction

Practical chemistry in the laboratory or in industry is usually performed in the liquid phase, whereas our chemical thinking, but also models or quantum chemical calculations, are nearly always limited to single molecules. To bridge the gap chemists "invented" the solvent effects, for example, they think of a reaction mechanism in the molecular picture and add then the solvent effects to explain the real behaviour in the liquid. For this reason solvent effects play an important role in many fields of chemistry.

It is this importance that made quantum chemists look for ways to include solvent effects in their calculations. One way, not to be discussed further here, is to include the solvent by some empirical reaction-field model. Such procedures are already part of some quantum chemical packages. However, to get better results, and if desired fully ab initio, we follow here a differ-

ent approach, which has been applied only in a few cases to date. In this approach a number of liquid configurations are obtained from simulations with empirical or ab initio force fields. In each configuration an atom or molecule of interest is selected randomly and neighbours are included to obtain clusters of desired size. Each cluster is then treated as a supermolecule in a quantum chemical calculation to get the desired property. Averaging over enough clusters yields the property in the liquid. The difference to the same property in the gas phase (usually the single molecule) finally gives the solvent effect.

This method was initially used to determine the solvent effect of vibrational frequencies in liquid water by Hermansson et al.[11] They employed pentamers of water obtained in Monte Carlo simulations and included further shells of water modelled by point charges. Related work was extended to ionic solutions and different potentials for water.[2, 3] Eggenberger et al.[4–6] applied it to the solvent shift of the nuclear quadrupole coupling of D and ^{17}O. Svishchev and Kusalik[7] used a similar method recently to examine the solvent effect of the proton chemical shift in water, utilising molecular dynamics simulations, but with a simple model instead of quantum chemical calculations to obtain chemical shifts. Chesnut and Rusiloski[8] then applied the full scheme to proton and ^{17}O NMR chemical shieldings, performing simulations with the program DISCOVER utilising the CFF-91 (class II) force field and calculating the NMR shifts with an ab initio coupled Hartree–Fock gauge including atomic orbitals (GIAO) calculations.

Experimental NMR chemical shieldings have been measured for nearly all molecules of interest in the liquid phase, but there is also an increasing number of compounds, for which gas-phase measurements were performed and, therefore, the solvent effect

[*] Dr. V. G. Malkin
Institute of Inorganic Chemistry, Slovak Academy of Science
Dubravska Cesta 9, SK-84236 Bratislava (Slovakia)
Fax: Int. code +(7)373-541
e-mail: malkin@savba.sk

O. L. Malkina
Computer Centre, Faculty of Natural Sciences, Comenius University
Mlynska Dolina CH-1, SK-84215 Bratislava (Slovakia)
Fax: Int. code +(7)729-064
e-mail: malkina@fns.uniba.sk

Prof. Dr. H. Huber, G. Steinebrunner
Institut für Physikalische Chemie der Universität Basel,
Klingelbergstr. 80, CH-4056 Basel (Switzerland)
Fax: Int. code +(61)267-3855
e-mail: huber@ubaclu.unibas.ch

is known. Several reviews have been published about gas-phase measurements.[9–11] For water, solvent effects of −4.26 ppm for protons[12, 13] and −36.1 ppm for ^{17}O[14, 15] were obtained.

Nowadays modern post-Hartree–Fock (see ref. [16–18] and references therein) and density-functional theory based approaches[19, 20] have reached such a level of accuracy that the remaining computational error is comparable to or smaller than solvent effects on NMR chemical shifts. It is even less when different conformations of the same molecule are compared.[21, 22] Therefore, a proper description and deeper understanding of solvent effects on chemical shifts become very topical.

In this paper we extend the work of Chesnut and Rusiloski[8] on water. Their results were not completely satisfactory, yielding gas–liquid shifts of −2.28 ppm for the proton and and −20.3 ppm for ^{17}O. Having applied only one force field, they point out that "…studies involving better documented force fields are desirable." In addition their results showed very large statistical errors. Here we try to find the reasons for the discrepancies from systematic methodical studies. We discuss the influence of rovibration, cluster size, potential, basis sets, quantum chemical method and temperature on the gas–liquid shift. A separation of intramolecular and intermolecular effects, as already described by Chesnut and Rusiloski, gives further insights.

Method and Calculations

Molecular dynamics simulations of water were performed within a microcanonical (constant NVE) ensemble. Flexible water molecules were placed in a cubic box with periodic boundary conditions. The velocities were scaled to yield the desired temperature. The densities were taken from experiment at standard pressure and the selected temperature.

The equations of motions were solved classically by the leap-frog version of the velocity-Verlet algorithm [23]. For the calculation of the force on every molecule, all other molecules were considered that were found inside a sphere around this molecule. The radius of this sphere, the cut-radius, was chosen to be 1 nm for the liquid and 6 nm for the gas. The interactions outside this sphere were only considered for the calculation of the energy long-range integral and the Coulomb forces were treated separately by the Ewald method [23]. The parameter κ, which determines the width of the screening charge distribution, was set to the typical value of $5/L$, where L is the side of the cubic box. This requires 122 k vectors.

Liquid water was simulated with 343 molecules using a time step of 0.25 fs. The equilibration took, at most, 10000 steps (i.e., 2.5 ps). During the equilibration the temperature was rescaled every 100 steps. After equilibration the simulation was run for another 10000 steps. Equally distributed snapshots were taken during this period. From each snapshot a molecule was selected randomly and nearest neighbours were determined to produce clusters of the desired size. The distance from the oxygen of the central molecule to the closest atom of the surrounding molecules was taken as criterion for the selection of the neighbours. For each cluster the chemical shielding in the central molecule was calculated quantum chemically (see below).

The simulations of gaseous water were performed with 64 molecules. This is sufficient, because the box length is very large due to the low density (a thousand times smaller than for the liquid). The large box length ensures the decay of the non-Coulombic forces to a negligible size within the box. The same time step as for the liquid is taken because the internal vibrations are almost the same. On the other hand, due to the longer mean free path a much longer simulation is required. The equilibration took about 200000 steps and the snapshots were taken over a range of another 100000 steps.

Both the gas and the liquid were studied with three different potentials at a temperature of 300 K. The three potentials were the ab initio potential by Lie and Clementi (LC) [24] and the two empirical potentials by Dang and Pettitt (DP) [25] and by Bopp et al. (BJH) [26]. In addition the LC potential was used for simulations at 350 K.

The LC potential has a four-site water molecule with one site on each atom and an additional site on the bisector of the H-O-H bond angle. The DP potential is a Lennard–Jones potential with an additional Coulomb interaction. The BJH potential uses the central-force model of Stillinger and Rahman [27] for the intermolecular potential. The intramolecular potential is the one of Carney et al. [28].

The calculations of chemical shifts were carried out with a modified version of the program deMon [29,30]. The sum-over-states density-functional perturbation theory (SOS-DFPT) approach used has been described in detail in ref. [19,20]. We use its LOC 1 approximation [19,20]. Perdew and Wang's exchange-correlation potential [31–33] was used for the chemical shift calculations. A "FINE" grid [19,20,29,30] with 32 radial points was employed throughout this study. The orbital basis set IGLO-III of Kutzelnigg et al. [34] was used. The sizes of the auxiliary basis sets [29,30] for the fit of exchange-correlation potential and charge density were 5,2 for oxygen and 5,1 for hydrogen (n,m designates n s functions and m spd shells). The individual gauge for localised orbitals (IGLO) procedure [34] employed orbitals localised by the Foster–Boys scheme [35]. The O 1 s orbitals were localised separately from the valence orbitals.

To study the influence of the quantum chemical method and the basis set applied, calculations for a selected cluster were performed with the coupled Hartree–Fock (CHF) GIAO method, utilising the Gaussian 94 program [36].

All statistical errors given in this paper are simple standard deviations. In the following the word "potential" is always used to mean "force-field" (and not exchange-correlation potential).

Results and Discussion

The chemical shift in the gas phase can be divided into an equilibrium value σ_e, that is, the shift calculated at the static equilibrium structure, and a rovibrational part $\Delta\sigma_{rv}$. Similarly, we divide the solvent effect on the shift into an intramolecular contribution due to the change of the structure of the molecule (including changes in the rovibrational part) $\Delta\sigma_i$ and an intermolecular or hydration contribution $\Delta\sigma_h$. The total absolute shielding in the liquid is then given by Equation (1), whereas the corresponding value for the gas phase is given by Equation (2). From Equations (1) and (2), the shift due to the solvent effects is then given by Equation (3). Note the different nomenclature

$$\sigma_{liq.} = \sigma_e + \Delta\sigma_{rv} + \Delta\sigma_i + \Delta\sigma_h \tag{1}$$

$$\sigma_{gas} = \sigma_e + \Delta\sigma_{rv} \tag{2}$$

$$\Delta\sigma_{solv} = \sigma_{liq} - \sigma_{gas} = \Delta\sigma_i + \Delta\sigma_h \tag{3}$$

used by Chesnut and Rusiloski,[8] who treat the sum of the present $\Delta\sigma_i + \Delta\sigma_{rv}$ as the rovibrational part in the liquid without detailed discussion of the role of $\Delta\sigma_{rv}$ in the gas phase. We will now start with a discussion of this latter contribution.

At the moment, a correct quantum mechanical treatment of the rovibrational contribution is not feasible for the liquid. For the gas phase, Fowler and Raynes[37] calculated quantum chemically $\Delta\sigma_{rv}$ values of −0.57 ppm for ^1H and −13.6 ppm for ^{17}O at 300 K. These values are quite large and far from negligible with respect to the shifts of interest. However, applying these values to the gas phase, while the liquid is treated classically, might even increase the error. Therefore, we assume that the rovibrational part is almost the same in both gas and liquid phase.

We would like to note here, that one cannot compare directly these small classical rovibrational corrections with quantum zero-order corrections, because the energy of the zero-order vibration is much higher than the energy of classical intramolecular rovibrations at room temperature. As a result, the geometry of a molecule averaged over quantum zero-order vibrational states differs more noticeably from the equilibrium structure than the geometry averaged over classical sampling at the temperatures investigated here.

In our molecular dynamics simulation of the liquid, all movements are treated classically, including the intramolecular rovibrations. Therefore, a classical sampling of these rovibrations is automatically performed, when clusters from the snapshots are

chosen. We decided to proceed fully analogically for the gas phase, that is, a gas of low density (55 mol m^{-3}) was simulated at the specific temperature and molecules randomly selected from the snapshots. The averaged results of the chemical shieldings are given in Table 1 and compared with the equilibrium shielding σ_e. Although, this classical treatment is not exact, we assume it is the most accurate method feasible at present.

Table 1. Chemical shieldings in the gas phase (average of 40 monomers) and the equilibrium value σ_e.

Potential	T/K	σ(H)/ppm	σ(O)/ppm
LC (ai)	300	30.95 ± 0.02	325.0 ± 0.5
BJH (emp.)	300	31.04 ± 0.02	325.8 ± 0.3
DP (emp.)	300	31.04 ± 0.01	326.1 ± 0.1
LC (ai)	350	31.02 ± 0.04	326.0 ± 0.7
σ_e		31.06	325.6

The small error bars for the DP potential are due to the harder bond in this potential (see Eggenberger et al.,[6] Table 1). The gas-phase shifts are very close to the equilibrium value σ_e, and the error introduced by applying σ_e instead of the gas-phase values, as Chesnut and Rusiloski did, is negligible compared to the remaining errors even at the higher temperature. However, we should be aware that we do not know how accurate the assumption is that classical and quantum chemical effects for the gas and the liquid compensate each other to the same extent. Having already calculated the gas-phase values, we applied them in this work.

In Table 2 the absolute chemical shieldings σ and the shifts for the liquid relative to the gas $\Delta\sigma$ are listed for different cluster sizes. Forty central molecules were selected randomly from the simulations and were used with their neighbours to yield clusters of size 1 and 9 for the quantum chemical calculations. In addition for ten of them, clusters of size 5 and 13 were produced to study dependence on the cluster size.

Table 2. Chemical shifts (ppm) in the liquid as a function of cluster size at 300 K (LC potential).

Size	No.	σ(H)	σ(O)	$\Delta\sigma$(H)	$\Delta\sigma$(O)
1	40	30.62 ± 0.07	319.0 ± 1.3	−0.33 ± 0.07	−6.0 ± 1.4
5	10	28.01 ± 0.44	293.9 ± 2.3	−2.94 ± 0.44	−31.0 ± 2.4
9	40	27.92 ± 0.20	288.6 ± 2.0	−3.03 ± 0.20	−36.4 ± 2.1
13	10	27.34 ± 0.39	286.9 ± 2.7	−3.61 ± 0.39	−38.1 ± 2.8
13 [a]	10			−3.22 ± 0.20	−37.6 ± 2.1

[a] Calculated from the sample of 40 clusters of size 9, and the differences between the 10 clusters of size 13 and the corresponding size 9 clusters (for details see text).

In the last line of Table 2 further values for the clusters of size 13 are given with smaller error limits. These values were obtained in the following way: For each cluster of size 13 the difference between its shielding and the shielding of the corresponding cluster of size 9 was calculated. Then, for these ten differences a mean of −0.19 ppm (±0.05 ppm) for ^{1}H and −1.23 ppm (±0.45 ppm) for ^{17}O was obtained. These numbers show that there is a clear decrease in the shieldings with increasing cluster size, as they are significantly different from zero (the numbers in parentheses being the standard deviations). Combining now these changes with the shieldings for the larger sample of 40 clusters of size 9 yields the values in the last line of Table 2, where the errors were obtained from a simple linear

error propagation. This last line of Table 2 gives then the best predictions of the gas–liquid shift obtained from the ab initio potential. The numbers agree reasonably with the experimental values of $\Delta\sigma_{exp}$(H) = − 4.26 and $\Delta\sigma_{exp}$(O) = − 36.1 ppm.

Figure 1 shows the relative shifts $\Delta\sigma$ versus the cluster size. Evidently, the hydrogen as well as the ^{17}O shifts level at a cluster size of 13. This cluster size therefore makes a good approximation for liquid water in calculations of chemical shifts.
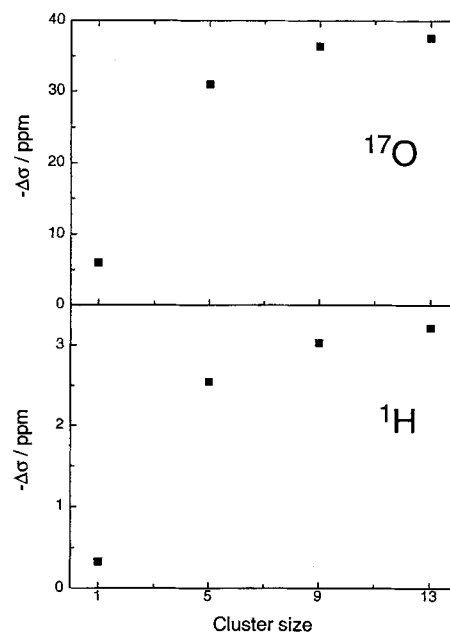

Fig. 1. ^{17}O (top) and ^{1}H (bottom) calculated shifts $\Delta\sigma$ versus cluster size showing the convergence of the shifts at clusters of size 13.

To study the influence of the force field, we applied in addition to the ab initio potential from Lie and Clementi (LC)[24] two empirical force fields, the one by Bopp, Jancso and Heinzinger (BJH)[26] and the one by Dang and Pettitt (DP).[25] In Table 3 we list the results obtained from 10 clusters of size 9. It should be pointed out, that all three force fields are dedicated force fields for water, whereas the force field used by Chesnut and Rusiloski is a general force field, not optimised specially for water. Therefore, if the results are force field dependent, we expect better results from these force fields.

Table 3. Chemical shifts obtained from 10 clusters of size 9 with different potentials.

Potential	T/K	σ(H)/ppm	σ(O)/ppm	$\Delta\sigma$(H)/ppm	$\Delta\sigma$(O)/ppm
LC (ai)	300	27.5 ± 0.4	288.1 ± 2.6	−3.4 ± 0.4	−36.8 ± 2.7
BJH (emp.)	300	28.0 ± 0.3	279.3 ± 4.4	−3.0 ± 0.3	−46.6 ± 4.4
DP (emp.)	300	28.3 ± 0.3	281.3 ± 2.3	−2.8 ± 0.3	−44.8 ± 2.3
CFF-91 (emp.) [a]	300			−2.3 ± 1.6	−20.3 ± 9.6
exp. [b]	300	25.79	307.9	−4.26	−36.1

[a] Values obtained by Chesnut and Rusiloski [8] with the program DISCOVER using the CFF-91 (class II) force field and ab initio coupled Hartree–Fock (GIAO) calculations. [b] From ref. [12–15].

Obviously, an agreement between experiment and calculation as good as that obtained with the LC ab initio potential could not be obtained with the empirical potentials. All three potentials seem to be treated equally in the literature, and we have no empirical criterion to favour one of them. We tried to find some

structural difference, analysing the g_{OH} pair distribution functions of the three potentials, to explain the results in Table 3, but did not succeed. That fact that we do not know why some potentials are better than others is a real handicap for the further application of this method to the calculation of solvent effects on chemical shieldings and efforts should be made to learn more about it. The agreement with experiment for the results with the two empirical potentials is far from perfect, but even the worst values are still an improvement on previous values,[8] given in Table 3 for comparison (CFF-91).

In Table 4 experimental and calculated shifts at 350 K are compared with the shifts at 300 K. Although, 40 clusters of size 9 were calculated (LC ab initio potential), the error could not be decreased to make a significant statement about temperature dependence. All we can say is that the calculated values do not contradict the experimental values.

Table 4. Temperature dependence of the chemical shifts obtained from 40 clusters of size 9.

Potential	T/K	σ(H)/ppm	σ(O)/ppm	$\Delta\sigma$(H)/ppm	$\Delta\sigma$(O)/ppm
LC (ai)	300	27.92 ± 0.20	288.6 ± 2.0	-3.03 ± 0.20	-36.4 ± 2.1
exp. [a]	300	25.79	307.9	-4.26	-36.1
LC (ai)	350	28.1 ± 0.2	288.4 ± 1.7	-2.9 ± 0.3	-37.6 ± 1.8
exp. [b]	350			-3.77	-33.7

[a] From ref. [12–15]. [b] From ref. [12,14].

In Table 5 we list the intramolecular part of the gas–liquid shift $\Delta\sigma_i$, obtained by subtracting the calculated shieldings for single molecules taken from the liquid and the gas simulation, respectively, and the intermolecular or hydration part $\Delta\sigma_h$, obtained by subtracting calculated shieldings for clusters of size 9 and size 1, both taken from the liquid simulation. Here we find a quite different picture than did Chesnut and Rusiloski, whose values are also given in Table 5 for comparison (CFF-91).

Table 5. Intra- und intermolecular effects on the shifts (ppm) at 300 K from clusters of size 9.

Potential	Sample size	Intramolecular		Intermolecular	
		$\Delta\sigma_i$(H)	$\Delta\sigma_i$(O)	$\Delta\sigma_h$(H)	$\Delta\sigma_h$(O)
LC (ai)	40	-0.33 ± 0.07	-6.0 ± 1.4	-2.70 ± 0.21	-30.4 ± 2.4
BJH (emp.)	10	-0.25 ± 0.06	-7.3 ± 1.0	-2.78 ± 0.34	-39.3 ± 4.5
DP (emp.)	10	-0.25 ± 0.06	-7.5 ± 1.0	-2.51 ± 0.35	-37.3 ± 2.5
CFF-91 (emp.)[a]	30	-0.34 ± 0.77	-8.2 ± 9.1	-1.93 ± 1.14	-12.1 ± 6.6

[a] Values obtained by Chesnut and Rusiloski [8] with the program DISCOVER using the CFF-91 (class II) force field and ab initio gauge including atomic orbitals (GIAO) calculations.

Whereas Chesnut and Rusiloski found the intra- and intermolecular contributions to be of similar size for oxygen, we find the latter to be larger by a factor 5 for all three potentials we applied. For hydrogen the corresponding factors are roughly 5 (Chesnut and Rusiloski) and 10 (our three potentials). The intramolecular part shows little dependence on the potential and is equal within error limits to the results of Chesnut and Rusiloski. The intermolecular part shows much larger fluctuations and is evidently the main source of the differences between the potentials applied in our study, as well as to the results of Chesnut and Rusiloski. In contrast to the D and ^{17}O quadrupole coupling constants, where the results hardly depend on the potential,[5, 6] the chemical gas–liquid shifts evidently depend

significantly on the quality of the intermolecular potential. In the D quadrupole coupling constant[4] only 40% of the solvent shift is due to intermolecular effects, whereas here it is 85%; this yields a partial explanation for the different dependence of the quadrupole couplings and the NMR chemical shifts on the quality of the intermolecular force field. Therefore, it will be important to improve the intermolecular potentials to get reliable NMR gas–liquid chemical shifts. Further work might show whether ab initio potentials are more reliable in this respect, since ab initio calculations of limited quality usually yield reliable structures while energetic properties are still of low quality, whereas effective empirical potentials fitted to energetic properties might not adequately reproduce the structure.

To study the influence of the quantum chemical method and the basis set on the calculation of the chemical shieldings in such clusters, additional calculations for one selected cluster were performed. The results are collected in Table 6. The value for the

Table 6. Shifts (ppm) relative to the equilibrium shielding σ_e for a selected cluster as a function of its size, calculated by different methods (GIAO or DFT) and basis sets (LD or IGLO-III).

	H [a]			^{17}O		
	GIAO LD [b]	GIAO IGLO-III	DFT IGLO-III	GIAO LD [b]	GIAO IGLO-III	DFT IGLO-III
σ_e	31.27	30.95	31.07	326.1	328.4	325.8
1	-0.15	-0.15	-0.13	-3.9	-4.1	-4.2
5	-1.40	-1.64	-1.94	-23.0	-25.2	-33.0
9	-1.13		-1.95	-24.6		-37.3
13	-1.43		-2.29	-23.0		-38.1

[a] Average of the two hydrogen values. [b] Locally dense basis set used by Chesnut and Rusiloski [8], namely, a 6-311 + +G(d,p) basis set on the central molecule and a 3-21G basis set on all other molecules.

rigid equilibrium structure and clusters of growing size around the selected monomer are shown. The first column (for H and ^{17}O, respectively) shows values obtained on the Hartree–Fock level with a locally dense basis set, as described by Chesnut and Rusiloski.[8] The third column gives the values obtained with the method applied in the present paper, whereas the second column gives values obtained with the present basis set, but on the Hartree–Fock level only. Evidently, the monomer values are of comparable quality in all three cases, but for the clusters and, hence, for the calculation of the solvent effect, there is a striking difference. A minor improvement in the present calculations is due to the larger basis set, but the outstanding improvement is due to the density-functional theory (DFT) method.

To study hydrogen bonds, Hinton et al. calculated the chemical shielding of hydrogen in ice clusters of different sizes.[38] However, it is difficult to judge the performance of the Hartree–Fock (HF) method in this study because the authors did not make a direct comparison with methods including electron correlation, and their comparison with experiment does not allow a definitive conclusion due to the large deviations between different experimental data.

In this context we would like to point out that in many cases electron correlation affects calculated chemical shifts noticeably. Significant progress in the development and application of the post-Hartree–Fock approaches to NMR chemical shift calculations during the last five years (see ref. [16–18] and references therein) have led to a new understanding of the importance of the correlation effects. It has been demonstrated that, even in cases where the correlation effects are expected to be small (water molecule, for example), the MP2 results are a significant improvement on the values calculated with HF (the

^{17}O shielding constant in water is 326.9 ppm calculated with HF and 344.8 ppm with MP2 (quadruple-zeta double polarization basis set)[116]).

In the past, the performance of the HF method in calculation of chemical shifts was overrated for the following reasons:
a) No post-HF results were available.
b) Medium-size basis sets were used (often there is an error cancellation due to insufficiently large basis sets and lack of electron correlation; see, e.g., ref. [16] and [39]).
c) Experimental data mostly consisted only of chemical shift measurements (i.e., the difference between the shielding constants in a reference molecule and in the molecule under study); this often leads to a partial compensation of the influence of correlation effects on calculated chemical shifts.

In addition, in some cases, the calculations on "difficult" molecules with strong electron correlation effects by means of the HF method were consciously avoided; this also contributed to the HF method being greatly overrated.

With the development of post-HF approaches for chemical shift calculations (mostly MP2 by J. Gauss[16]) the interest in calculations at the HF level decreased. However, since the MP2 approach for chemical shift calculations is even more expensive than HF, there is a growing interest in alternatives to chemical shift calculations.

Density-functional theory[40, 41] provides such an alternative by inclusion of correlation effects in an approximate manner with modest computational costs. Even though the DFT method is not a universal tool and has its own shortcomings, it is a well-accepted method for studying large-scale molecules, especially with nonnegligible correlation effects. The recently developed SOS-DFPT method for chemical shift calculations[19, 20] leads to superior results compared to those obtained with HF and is almost as good as the MP2 approach[20, 42] for carbon chemical shifts in systems where correlation is not extremely strong. Moreover, SOS-DFPT gives reasonable results even for systems with very strong correlation effects such as the ozone molecule and many transition metal complexes where the HF and even the MP2 method fail completely [20, 43].

The SOS-DFPT method has already been successfully applied to the study of intermolecular interactions in the α-glycine crystal,[44] in the gramicidin channel[45] and in other biosystems.[46] However, it is still difficult to judge the accuracy of the SOS-DFPT method in this particular case, because there might be an error cancellation due to the geometries provided by molecular dynamics simulation and the method for chemical shift calculations. Therefore, at present we only can conclude that the SOS-DFPT approach leads to a better agreement with experiment; we do not have enough data to interpret this fact further. However, based on our experience, we believe that SOS-DFPT provides a better description of the influence of hydrogen bonding on chemical shift than the HF method.

For practical purposes it might be interesting to compare the cpu times used for the different calculations. For clusters of size 5, the times on a workstation and the number of contractions were 14 min/88 contractions (CHF-GIAO/LD, Gaussian94), 790 min/275 contractions (CHF-GIAO/IGLO-III, Gaussian94) and 119 min/275 contractions (SOS-DFPT/IGLO-III, deMon).

To calculate accurate solvent effects on the NMR chemical shieldings, it is evidently crucial to apply an accurate quantum chemical method with a large enough basis sets. Apart from better potentials, the results should be improved by calculating larger samples of clusters, rather than by going beyond the cluster size of 13, as the statistical error is larger than the estimated error due to the limited cluster size.

Conclusions

The solvent effects on the NMR chemical shieldings of the proton and ^{17}O in water have been calculated by a combination of molecular dynamics simulations and quantum chemical calculations. The values calculated for the gas-liquid shifts with the ab initio potential, namely, -3.2 ± 0.2 ppm for ^{1}H and -37.6 ± 2.1 ppm for ^{17}O, compare favourably with the experimental values of -4.26 (^{1}H) and -36.1 ppm (^{17}O). However, in contrast to solvent effects of nuclear quadrupole couplings the results depend heavily on the applied force field and the influence of distant solvent molecules is larger. The latter problem is taken care of by selecting larger clusters from the liquid, leading to more time-consuming quantum chemical calculations. However, it is not an easy task to discriminate between the various force fields reported in the literature, in order to find the best one. A good choice of the quantum chemical method and the basis sets for the calculation of the shieldings is crucial. Whereas for a single water molecule the calculations on the HF and the DFT level give similar results, they diverge increasingly with larger clusters. This shows, in our opinion, that electron correlation (partially included in DFT) is important for the intermolecular induced shifts.

[1] K. Hermansson, S. Knuts, J. Lindgren, *J. Chem. Phys.* **1991**, *95*, 7486–7496.
[2] L. Ojamäe, K. Hermansson, M. Probst, *Chem. Phys. Lett.* **1992**, *191*, 500–506.
[3] M. J. Wojcik, K. Hermansson, J. Lindgren, L. Ojamäe, *Chem. Phys.* **1993**, *171*, 189–201.
[4] R. Eggenberger, S. Gerber, H. Huber, D. Searles, M. Welker, *J. Chem. Phys.* **1992**, *97*, 5898–5904.
[5] R. Eggenberger, S. Gerber, H. Huber, D. Searles, M. Welker, *Mol. Phys.* **1993**, *80*, 1177–1182.
[6] R. Eggenberger, S. Gerber, H. Huber, D. Searles, M. Welker, *J. Comput. Chem.* **1993**, *14*, 1553–1560.
[7] I. M. Svishchev, P. G. Kusalik, *J. Am. Chem. Soc.* **1993**, *115*, 8270–8274.
[8] D. B. Chesnut, B. E. Rusiloski, *J. Mol. Struct. (Theochem)* **1994**, *314*, 19–30.
[9] G. Govil, *Appl. Spectrosc. Rev.* **1973**, *7*, 47–78.
[10] C. J. Jameson, *Bull. Magn. Reson.* **1980**, *3*, 3–28.
[11] C. J. Jameson, *Chem. Rev.* **1991**, *91*, 1375–1395.
[12] J. C. Hindman, *J. Chem. Phys.* **1966**, *44*, 4582–4592.
[13] W. T. Raynes, *Nucl. Magn. Reson.* **1978**, *7*, 1–25.
[14] A. E. Florin, M. Alei, *J. Phys. Chem.* **1967**, *47*, 4268–4269.
[15] W. T. Raynes, *Mol. Phys.* **1983**, *49*, 443–447.
[16] J. Gauss, *J. Chem. Phys.* **1993**, *99*, 3629.
[17] J. Gauss, *Chem. Phys. Lett.* **1994**, *229*, 198.
[18] J. Gauss, J. F. Stanton, *J. Chem. Phys.* **1995**, *102*, 251.
[19] V. G. Malkin, O. L. Malkina, M. E. Casida, D. R. Salahub, *J. Am. Chem. Soc.* **1994**, *116*, 5898.
[20] V. G. Malkin, O. L. Malkina, L. A. Eriksson, D. R. Salahub in *Modern Density Functional Theory: A Tool for Chemistry; Theoretical and Computational Chemistry*, Vol. 2 (Eds.: J. M. Seminario, P. Politzer), Elsevier, Amsterdam, **1995**.
[21] H. M. Sulzbach, P. von R. Schleyer, H. F. Schaefer, *J. Am. Chem. Soc.* **1994**, *116*, 3967.
[22] H. M. Sulzbach, P. von R. Schleyer, H. F. Schaefer, *J. Am. Chem. Soc.* **1995**, *117*, 2632–2637.
[23] M. P. Allen, D. J. Tildesley, *Computer Simulation of Liquids*, Clarendon Press, Oxford, **1987**.
[24] G. C. Lie, E. Clementi, *Phys. Rev. A* **1986**, *33*, 2679–2693.
[25] L. X. Dang, B. M. Pettitt, *J. Phys. Chem.* **1987**, *91*, 3349–3354.
[26] P. Bopp, G. Jancsó, K. Heinzinger, *Chem. Phys. Lett.* **1983**, *98*, 129–133.
[27] F. H. Stillinger, A. Rahman, *J. Chem. Phys.* **1978**, *68*, 666–670.

[28] G. D. Carney, L. A. Curtiss, S. R. Langhoff, *J. Mol. Spectrosc.* **1976**, *61*, 371–381.

[29] D. R. Salahub, R. Fournier, P. Mlynarski, I. Papai, A. St-Amant, J. Ushio in *Density Functional Methods in Chemistry* (Eds.: J. Labanowski, J. Andzelm), Springer, New York, **1991**.

[30] A. St-Amant, D. R. Salahub, *Chem. Phys. Lett.* **1990**, *169*, 387.

[31] J. P. Perdew, Y. Wang, *Phys. Rev. B* **1992**, *45*, 13244.

[32] J. P. Perdew in *Electronic Structure of Solids* (Eds.: P. Ziesche, H. Eischrig), Akademie Verlag, Berlin, **1991**.

[33] J. P. Perdew, J. A. Chevary, S. H. Vosko, K. A. Jackson, M. R. Pederson, D. J. Singh, C. Fiolhais, *Phys. Rev. B* **1992**, *46*, 6671.

[34] W. Kutzelnigg, U. Fleischer, M. Schindler in *Deuterium and Shift Calculation*; *NMR-Basic Principles and Progress*, Vol. 23 (Eds.: P. Diehl, E. Fluck, H. Günther, R. Kosfeld, J. Seelig), Springer, Heidelberg, **1990**.

[35] S. F. Boys in *Quantum Theory of Atoms, Molecules and the Solid State* (Ed. P. O. Löwdin), Academic Press, New York, **1966**.

[36] Gaussian 94, Revision B.2, M. J. Frisch, G. W. Trucks, H. B. Schlegel, P. M. W. Gill, B. G. Johnson, M. A. Robb, J. R. Cheeseman, T. A. Keith, G. A. Petersson, J. A. Montgomery, K. Raghavachari, M. A. Al-Laham, V. G. Zakrzewski, J. V. Ortiz, J. B. Foresman, J. Cioslowski, B. B. Stefanov, A. Nanayakkara, M. Challacombe, C. Y. Peng, P. Y. Ayala, W. Chen, M. W. Wong, J. L. Andres, E. S. Replogle, R. Gomperts, R. L. Martin, D. J. Fox,

J. S. Binkley, D. J. Defrees, J. Baker, J. P. Stewart, M. Head-Gordon, C. Gonzalez, J. A. Pople ; Gaussian Pittsburgh PA, **1995**.

[37] P. W. Fowler, W. T. Raynes, *Mol. Phys.* **1981**, *43*, 65–82.

[38] J. F. Hinton, P. Guthrie, P. Pulay, K. Wolinski, *J. Am. Chem. Soc.* **1992**, *114*, 1604–1605.

[39] K. Wolinski, C.-L. Hsu, J. F. Hinton, P. Pulay, *J. Chem. Phys.* **1993**, *99*, 7819–7824.

[40] R. G. Parr, W. Yang, *Density-Functional Theory of Atoms and Molecules*, Oxford University Press, Oxford, **1989**.

[41] *Modern Density Functional Theory: A Tool for Chemistry*; *Theoretical and Computational Chemistry*, Vol. 2 (Eds.: J. M. Seminario, P. Politzer), Elsevier, Amsterdam, **1995**.

[42] C. Maerker, P. von R. Schleyer, D. R. Salahub, O. L. Malkina, V. G. Malkin, unpublished results.

[43] M. Kaupp, *Conference on Computational Chemistry in Mariapfarr (Austria)* **1995**.

[44] V. G. Malkin, O. L. Malkina, D. R. Salahub, *J. Am. Chem. Soc.* **1995**, *117*, 3294–3295.

[45] T. B. Woolf, V. G. Malkin, O. L. Malkina, D. R. Salahub, B. Roux, *Chem. Phys. Lett.* **1995**, *239*, 186.

[46] D. Case, private communication.